Exotic crystal superstructures of colloidal crystals in confinement

Ana Barreira Fontecha and Hans Joachim Schöpe
Institut für Physik, Johannes Gutenberg-Universität Mainz, Staudingerweg 7, D-55128 Mainz, Germany
(Received 30 November 2007; revised manuscript received 4 March 2008; published 4 June 2008)

Colloidal model systems have been used for over three decades for investigating liquids, crystals, and glasses. Colloidal crystal superstructures have been observed in binary systems of repulsive spheres as well as oppositely charged sphere systems showing structures well known from atomic solids. In this work we study the structural transition of colloidal crystals under confinement. In addition to the known sequence of crystalline structures, crystal superstructures with dodecagonal and hexagonal symmetry are observed in one component systems. These structures have no atomic counterpart.

DOI: 10.1103/PhysRevE.77.061401 PACS number(s): 82.70.Dd, 42.70.Qs, 68.65.Cd, 78.67.Pt

Colloids have become an important model system to study the physical processes in liquids, solids, and on surfaces mapping the physical properties of atomic systems on another time and length scale. Charged and hard sphere suspensions have been used over three decades investigating the structural and dynamic properties of liquids, crystals, and glasses as well as crystallization and the glass transition. These studies were performed in bulk systems, in one- and two-dimensional systems and in the transition from two to three dimensions [1–9]. Crystal superstructures have been observed in binary systems of repulsive spheres as well as oppositely charged sphere systems showing structures known from atomic solids [10–15]. In general crystal superstructures in the bulk are formed in multicomponent systems and are described by a superposition of two or more Bravais lattices. We here present crystal superstructures observed in one component colloidal model systems under confinement, which have no atomic counterpart.

Confined geometries are ideally suited for investigating the transition regime between two and three dimensions. Confining a colloidal suspension in a narrow gap between two glass plates, the restriction of motion perpendicular to the wall can be controlled via particle-wall interactions and the separations of the plates. Pieranski *et al.* [9] were one of the first groups investigating the behavior of colloidal particles in wedge geometries. They found a sequence of transitions with increasing the cell height, having the general form

$$n\Delta \rightarrow (n+1)\square \rightarrow (n+1)\Delta, \tag{1}$$

where n denotes the number of layers and Δ and $\square$ denote triangular or square symmetry, respectively. Both packings derive from placing the fcc-(111) or hcp-(001) and fcc-(100) face of the close-packed structures parallel to the confining walls. Subsequently theoretical predictions and experiments evidenced the existence of intermediate structures in the transition from $n\Delta \rightarrow (n+1)\square$ as well as in the $(n+1)\square \rightarrow (n+1)\Delta$ transition optimizing the packing efficiency: buckling (B), rhombic (R), and prism phases (P) can be observed [16–18]. Recently a hexagonal close-packed structure (hcp $\perp$) with the crystallographic planes (210) oriented parallel to the cell walls has been presented for $n>2$ [19]. This structure appears in the transition $n\Delta \rightarrow (n+1)\square$ and is observed to coexist with nP and $(n+1)\square$. In this paper we present arrangements of particles also present in the $n\Delta \rightarrow (n+1)\square$ transition. We observe two different crystal superstructures up to eight layers thick.

For our experiments we used commercially available electrostatically stabilized carboxylate modified latex spheres (IDC Batch No. 2149) of diameter $2a=1.1$ μm with a size polydispersity of 2.1%. The stock suspension is deionized using ion exchange resins for several weeks. After that the suspension is prepared with carbonate saturated ultrapure water ($c=5.6$ μmol/l) and the samples were left in contact with air to obtain saturation with airborne carbonate. The final volume fraction of the suspension is 1%. The saturation process is conveniently and accurately monitored by means of the conductivity. In this way salt gradients during the experiment can be avoided. The wedge cells used consist of two glass slides $(25\times 75\times 1)$ mm^3 glued water tight with a 50 μm spacer included at one side leading to wedge angle in the order of 10^{-4} rad. Before use the glass slides were cleaned with hot sulfuric acid, washed with ultrapure water, and dried in a dust-free stream of argon. The plates are slightly negatively charged which avoids sticking of particles on the glass plates. In the top plates are two holes to introduce the suspension. After filling in the suspension the cell is completely sealed. Just after filling the cell we observed a homogeneous particle density throughout the sample. Several hours later the particles are observed to migrate slowly (within a few days) to the narrow side of the cell and assemble into different crystal structures at growth rates of about 1 μm/h. We carefully checked several possible experimental artifacts, such as contamination by a local source of electrolyte, evaporation, gradients of temperature or of solvent composition, and gravity, which can all be excluded. Although this behavior is not completely understood we think that it can be due to increased self-screening in the narrow part of the cell as the counterion concentration stemming from the particles and the cell walls is increasing with decreasing wall distance.

The samples are observed with an inverted optical microscope (Leica DM IRB/E) using low (20× and 40×) and high magnification objectives (PL Fluotar L 63×/0.7 corr PH2 ∞/0.1-1.3/C, Leitz). The objective focal plane can be moved through the sample by a piezoelectric drive (PI, Germany). This allowed us to determine the particle position in z direction for $n<5$ with an accuracy of ± 200 nm. For higher layer number the uncertainties due to poor imaging are too

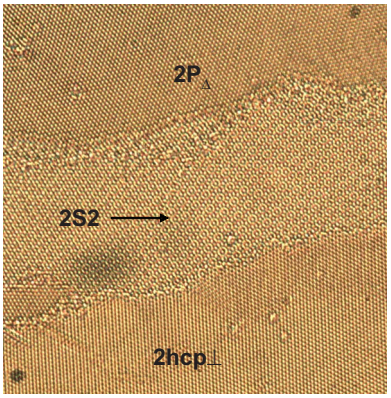

FIG. 1. (Color online) Optical micrograph of the observed superstructures coexisting with other structures as indicated. Picture size 225×225 μm^2.

large to obtain meaningful data. Fourier images were obtained in the conoscopic mode using an additional Bertrand lens to image the back focal plane of the objectives. In order to obtain sharp images of the diffraction patterns we reduce the radius from both the field and iris diaphragms. We also added in the optical light path an interference filter ($\lambda = 488$ nm, $\Delta\lambda_{FWHM} = \pm 10$ nm, LOT-Oriel, Germany) in order to have quasimonocromatic light. Images were recorded with a 3.5 Mpix color digital camera (OTX2, 3.3FZK, La Vision, Germany) and stored for later evaluation.

Using the particle coordinates obtained from the real space pictures we are able to construct a real space model of the observed crystal superstructures. As the uncertainties in the z direction are quite large we assumed that the structure is following the maximum packing criterion leading to unique positions in the z direction. From the constructed real space lattice we calculated the corresponding scattering pattern using special software for crystallography (CaRIne) and a self-written routine in MATHEMATICA taking the Mie-form factor of the spheres into account.

All our samples show the known sequence of crystalline structures as described in the Introduction. In addition we observe in the $n\Delta \rightarrow (n+1)\square$ transition two different crystal superstructures (we will call them in the following $nS1$ and $nS2$) coexisting with $n$hcp$\perp$ and $nP\Delta$. In contrast with the extended domains of $n\Delta$, nhcp$\perp$, $nP\Delta$, and $(n+1)\square$ only small domains of these superstructures (40-500 μm^2) can be found (Fig. 1). While $n\Delta$ converts continuously to $n$hcp$\perp$ or $nP\Delta$ there is no continuous and smooth transition to these superstructures. There is always an abrupt transition from $n\Delta$, $n$hcp$\perp$, or $nP\Delta$ to nS. The domain boundaries of nS are of small width between one and four particle layers. Further a smooth transition between the superstructures $S1$ and $S2$ is possible. These structures are present in all our confined samples independent of the number of layers, but these structures are not as stable as other intermediates: The structures are commonly destroyed during drying of the sample. Only after a careful and slow drying process over several weeks are the structures maintained, but with a significant loss of periodicity.

Figures 2 and 3 show two different configurations of the ordered superstructure for the transition $2\Delta \rightarrow 3\square$. We propose an ideal superstructure system for each arrangement based on the measurements done with high-resolution optical microscopy [Figs. 2(a) and 3(a)] and Fourier microscopy [Figs. 2(b) and 3(b)]. The first layer of $nS1$ is a hexagonal layer [Fig. 2(c) top, blue spheres] of a hexagonal unit cell with lattice constants a, b, and c. In the second layer (red spheres) the particles are arranged in a hexagon centered above a particle in the first layer. However, the orientation of these hexagons relative to each particle in the first layer is constant, so neighboring hexagons form squares. This means that each pair of neighboring hexagons in the layer is a pair of twins, divided by a twin grain boundary. Therefore the

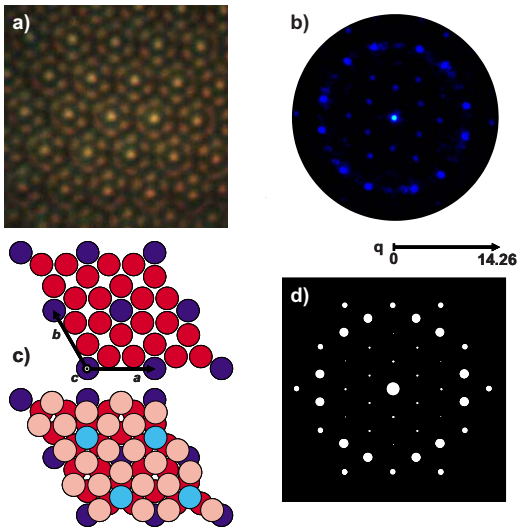

FIG. 2. (Color online) (a) High-resolution optical micrograph of $2S1$ (picture size 20×20 μm^2), (b) corresponding Fourier micrographs of $2S1$, (c) on top, top view of the first two layers of $nS1$, bottom, top view of a model for $2S1$, and (d) corresponding scattering pattern based on the model shown in (c).

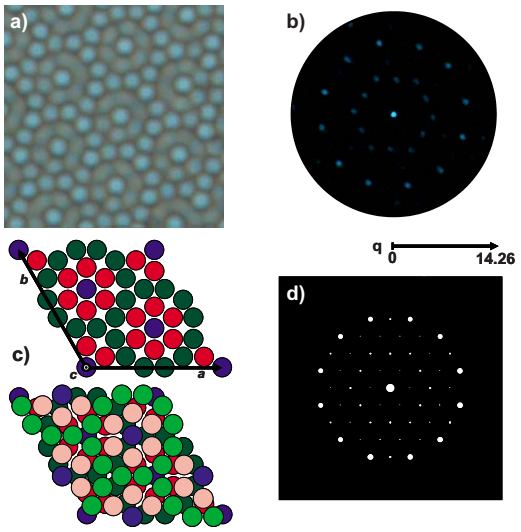

FIG. 3. (Color online) (a) High-resolution optical micrograph of $2S2$ (picture size 15×15 μm^2), (b) corresponding Fourier micrographs of $2S2$, (c) on top, top view of the first two layers of $nS2$, bottom, top view of a model for $2S2$, and (d) corresponding scattering pattern based on the model shown in (c).

construction principle of this layer can also be interpreted as a regular arrangement of twin grain boundaries. The vertical shift between the first and the second layer increases with the cell height up to $\Delta z \approx 1/10c$, where c is the lattice constant of the hcp unit cell in the z direction. Each subsequent layer is shifted pairwise laterally by $a=2/3$ and $b=1/3$ [Fig. 2(c) bottom]. The vertical shift is a function of the cell height and the minimum shift is 1.633 particle radii. The calculated scattering pattern [Fig. 2(d)] matches the experimental one [Fig. 2(b)] quite well. There are some small deviations around a scattering vector of $q \approx 10.3$ μm^{-1} which could stem from dislocations in the second layer. The obtained experimental packing fraction is observed to be around 0.5 whereas the theoretical one for an ideal hard sphere system is about 0.7 in the bulk and about 0.62 for two layers in confinement.

The structure of $nS2$ is more complex (Fig. 3). Here in the first layer of the superstructure [Fig. 3(c) top, blue and dark green spheres] 12 particles (dark green) are forming a regular dodecagon around one center particle (blue). The center particles are located on a hexagonal layer of a hexagonal unit cell with lattice constants a, b, and c. The second layer consists of hexagons (red spheres) centered inside the dodecagon and shifted as a function of the cell height up to $\Delta z \approx 1/15c$, where c is the lattice constant of the hcp unit cell in the z direction. A periodic arrangement along the c axis is obtained by shifting additional layers pairwise laterally by $a=1/3$ [Fig. 3(c) bottom] and vertically by more than 1.633 particle radii. The calculated scattering pattern [Fig. 3(d)] reflects the experimental one [Fig. 3(b)]. Again we find an experimental packing fraction around 0.5. The theoretical volume fraction for the bulk structure is about 0.71 and for a two layer system about 0.64.

In summary we have studied a colloidal system under confinement in a wedge geometry. The experiments reveal the existence of superstructures in the transition $n\Delta \rightarrow (n+1)\square$ with two different possible configurations. These structures, not predicted in theoretical ground state calculations for hard spheres in confinement, show that the structural transitions of spheres in confinement are much more complex than previous studies suggest. We hope that this study will stimulate further theoretical investigations for a quantitative comparison.

In addition our findings show crystal superstructures not known from atomic systems. Crystal superstructures in atomic systems can always be described by a superposition of Bravais lattices, which is also the case in superstructures presented here. In addition, superstructures in atomic systems are only formed where there are nonsymmetric interactions (multicomponent systems). By contrast, for the experiments reported here, all particles have nearly the same interaction potential with spherical symmetry. We speculate that the superstructures could be formed by an intergrowing of domains of different structures ($n\Delta$, $n\mathrm{hcp}\perp$, $nP\Delta$) oriented in different directions.

Further these structures have interesting properties for photonics, showing Bragg spots at low and high q, indicating complex photonic band structures with multiple stop bands possible as a function of the scattering contrast.

We thank H. Löwen and R. Goldberg for fruitful discussions, and acknowledge the financial support of DFG (Grant No. SFB TR6), Forschungsfond, and MWFZ, Mainz.

[1] P. N. Pusey and W. van Megen, Nature (London) **320**, 340 (1986).
[2] W. van Megen, Transp. Theory Stat. Phys. **24**, 1017 (1995).
[3] V. J. Anderson and H. N. W. Lekkerkerker, Nature (London) **416**, 811 (2002).
[4] P. Bartlett and W. van Megen, in *Granular Matter*, edited by A. Mehta (Springer, New York, 1994).
[5] H. J. Schöpe, G. Bryant, and W. van Megen, Phys. Rev. Lett. **96**, 175701 (2006).
[6] K. Zahn, A. Wille, G. Maret, S. Sengupta, and P. Nielaba, Phys. Rev. Lett. **90**, 155506 (2003).
[7] C. Lutz *et al.*, J. Phys.: Condens. Matter **16**, S4075 (2004).
[8] C. Bechinger, Curr. Opin. Colloid Interface Sci. **7**, 204 (2002).
[9] P. Pieranski, L. Strzelecki, and B. Pansu, Phys. Rev. Lett. **50**, 900 (1983).
[10] S. Yoshimura and S. Hachisu, Prog. Colloid Polym. Sci. **68**, 59 (1983).
[11] S. Hachisu, Phase Transit. **21**, 243 (1990).
[12] T. Okubo, J. Chem. Phys. **93**, 8276 (1990).
[13] P. Bartlett, R. H. Ottewill, and P. N. Pusey, J. Chem. Phys. **93**, 1299 (1990).
[14] A. B. Schofield, P. N. Pusey, and P. Radcliffe, Phys. Rev. E **72**, 031407 (2005).
[15] M. E. Leunissen *et al.*, Nature (London) **437**, 235 (2005).
[16] S. Neser, C. Bechinger, P. Leiderer, and T. Palberg, Phys. Rev. Lett. **79**, 2348 (1997).
[17] H. J. Schöpe *et al.*, Langmuir **22**, 1828 (2006).
[18] A. Fortini and M. Dijkstra, J. Phys.: Condens. Matter **18**, L371 (2006).
[19] A. B. Fontecha, T. Palberg, and H. J. Schöpe, Phys. Rev. E **76**, 050402(R) (2007).